NUMERICAL SOLUTION FOR THE DROPLET COMBUSTION IN MICROGRAVITY

Mariovane S. Donini, mariovanedonini@alunos.unipampa.edu.br[1]
Cesar F. C. Cristaldo, cesarcristaldo@unipampa.edu.br[1]
Fernando. F. Fachini, fachini@lcp.inpe.br[2]

[1]Grupo de Fenômenos de Transporte Avançado - FENTA, Universidade Federal do Pampa, 97546-550 Alegrete-RS, Brazil
[2]Grupo de Mecânica de Fluidos Reativos/LCP, Instituto Nacional de Pesquisas Espaciais,12630-000 Cachoeira Paulista-SP, Brazil

Abstract:
In the present work, combustion of an isolated fuel droplet at different ambient temperatures are examined numerically in order to analyze the effect of buoyancy force on the flame. Generally, fuel droplets in combustion devices are so small that the influence of buoyancy force on vaporization and combustion of droplets is negligible. On the other hand, fuel droplets in experimental devices are affected by the buoyancy force due to their diameters around or more than 1 mm. To reduce the buoyancy effects, expensive experimental studies are performed in microgravity ambient (drop-tower or out of space). In normal-gravity conditions, the buoyancy force is induced by gradient of temperature on ambient atmosphere. The buoyancy is positive in regions of hot gases and negative in regions of cold gases compared with the ambient atmosphere gas. The hot gases move upward and cold gases downward. Playing with the positive buoyancy force of hot gases around the flame and with the negative (cold) buoyancy force of cold gases around the droplet via ambient atmosphere temperature, it is possible to modified the flame shape. At high temperature ambient the condition of spherical flame shape is verified, this method could be used to simulate droplet combustion in microgravity condition.
Keywords: *Droplet Combustion, Microgravity, Natural Convection*

1. INTRODUCTION

Isolated droplet combustion experiments is of practical interest. Since the liquid fuels possess high energy content per unit mass and are relatively safe to store and transport, they are of great interest in many practical applications that as electric power production, industrial burners, space propulsion or diesel engines. All of these applications involve a dispersed liquid phase species in the form of a large number of small droplets. Under this condition, the small droplets ($1 - 100\mu m$ diameter) are not greatly affected by buoyancy. On the other hand, experiments in laboratory are performed with large droplets, (diameter of the order of millimeter). The effects of buoyancy in these experiments (for large droplets) compromise seriously our capabilities to carry out experiments, which are needed to advance our understanding of flame phenomena on droplet combustion. To avoid buoyancy effects, the droplet combustion is submitted on a microgravity environment, thus a spherically symmetrical combustion is observed. An advantage of the spherical symmetry is that only one spatial dimension enters the description of the combustion process, so that one-dimensional time-dependent conservation equations apply, facilitating both computational and theoretical descriptions of the combustion (Dietrich *et al.*, 2014). Despite the simplifications afforded by spherical symmetry, many complexities remain in microgravity studies of droplet combustion. Among them are time-dependent liquid-phase phenomena, soot production, radiant energy transfer and effects of multicomponent fuels.

There are many experiments to evaluate microgravity combustion, like studies utilizing drop-tower facilities, parabolic aircraft and extended duration testing on orbiting facilities (Eigenbrod, 1999). These experiments provide vital information concerning how fires behave in microgravity and how fire safety on spacecraft can be enhanced (King and Ross, 1998). Dietrich *et al.* (1996) performed droplet combustion experiments in space-based platforms aboard the space shuttle Columbia with droplets initial diameters of 3.5 mm and 5.2 mm. Manzello *et al.* (2000) realized experiments to analyze the burning of large n-heptane droplets in microgravity. The experiments were performed at the Japan Microgravity Center (JAMIC) drop shaft. The JAMIC facility is the longest drop shaft in the world and provides 10 seconds of gravity levels less than 10^{-5}g. Choi and Kyeong-Okk (1996) analyzed n-heptane droplets burning under microgravity conditions for droplet diameters ranging from 0.8 mm to 1.8 mm and Yozgatligil *et al.* (2007) investigated the large ethanol droplets (diameters ranging from 1 to 3 mm) under microgravity conditions, both in the 2.2s droptower at the NASA Glenn Research Center. The results suggested that would require larger droplets to better describe the effects of sooting and radiation in their experiments. However, the duration of the microgravity observation time available in the 2.2 s droptower was insufficient to extend the investigation for larger droplets. Larger droplets require longer preparation time for droplet formation, deployment, ignition, and the oscillation decay period caused by these procedures. Chauveau *et al.* (2011) examined experimentally n-decane droplet vaporization. Two sets of experiments were performed, one in normal gravity and another in microgravity conditions. The latter were realized using the parabolic flights aboard the A300 Airfcraft of CNES (The French Space Agency).

Numerical studies on fuel droplets under normal and microgravity are also available in the literature. Jiang *et al.* (1995) analyzed numerically multiple flame configurations of a convective n-octane fuel droplet at various Damköhler and Reynolds numbers and diameter of 0.1 mm. Pope and Gogos (2005) investigated a n-heptane fuel droplet extinction

due to forced convection with numerical simulation for droplet sizes ranging from 0.1 mm to 15 mm and a wide range of ambient temperatures.

Considering the difficult and the cost for large droplet combustion experiments in microgravity, in the present study, an isolated fuel droplet at different ambient temperatures are examined numerically in order to analyze the effect of buoyancy force on the flame and be able to implement less expensive ground based experiments. Recalling that, the increase on the temperature of ambient results in decrease of gradient on temperature on the gas-phase, resulting in decrease on buoyancy force.

2. MATHEMATICAL FORMULATION

In the present work, the physical model considers a porous sphere (named droplet) with gaseous fuel being fed from its interior to its surface. The droplet is placed in a ambient under normal gravity $g = 9.8\, m/s^2$. In the present model, all the thermo-physical properties are constants, with the exception the density that is assumed as a function of the temperature through the ideal gas law. In addition, the radial velocity u_r of vapor fuel injection is considered as a constant. The pressure is assumed constant. The schematic diagram of computation domain is shown in Fig. 1.

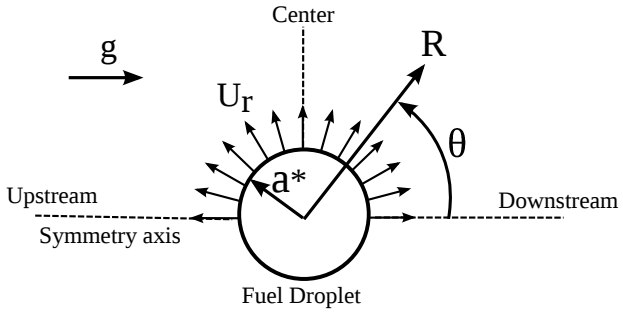

Figure 1: **Problem schematic (constant radius droplet with fuel injection).**

The dimensionless variables used in the analysis are defined as

$$T \equiv \frac{T^*}{T_b^*}, \quad \rho \equiv \frac{\rho^*}{\rho_b^*}, \quad y_F \equiv y_F^*, \quad y_O \equiv \frac{y_O^*}{Y_{O\infty}^*}, \quad r \equiv \frac{r^*}{\mathrm{a}^*}, \quad t \equiv \frac{t^*}{t_c^*}, \quad u_r \equiv \frac{u_r^*}{u_c^*}, \quad u_\theta \equiv \frac{u_\theta^*}{u_c^*}$$

The superscript "*" stands for variables in dimensional form and the subscript b and ∞ stand for boiling condition and ambient condition (far from the droplet), respectively. The variables T, ρ, y_F, y_O are temperature, density, fuel mass fraction, oxidant and mass fraction, respectively. The radial coordinate r^* is nondimentionalized by the constant droplet radius a*,the time t^* by estimated heating time $t_c^* = \mathrm{a}^*/u_c$, α_∞ is the thermal diffusivity $\alpha_\infty = k_{g\infty}/c_p\rho_\infty^*$, in which k_∞^* is the thermal conductivity and c_p^* is the specific heat. The velocity is nondimentionalized by the diffusion velocity of gas-phase $u_c \equiv \alpha_\infty^*/\mathrm{a}^*$.

The spherical coordinate with azimuthal symmetry (r, θ) are used in the formulation of the problem. The governing equations include the conservation equations for mass, momentum in the radial and polar directions, mixture fraction, excess enthalpy and the equation of state:

$$\frac{\partial(r^2\sin\theta\rho)}{\partial t} + \frac{\partial(r^2\sin\theta\rho u_r)}{\partial r} + \frac{\partial(r\sin\theta\rho u_\theta)}{\partial\theta} = 0 \tag{1}$$

$$\frac{\partial(r^2\sin\theta\rho u_r)}{\partial t} + \frac{\partial(r^2\sin\theta\rho {u_r}^2)}{\partial r} + \frac{\partial(r\sin\theta\rho u_\theta u_r)}{\partial\theta} - r\sin\theta\rho {u_\theta}^2 = \\ + Sg_r + \frac{\partial}{\partial r}\left(r^2\sin\theta\tau_{RR}\right) + \frac{\partial}{\partial\theta}\left(r\sin\theta\tau_{R\theta}\right) - r\sin\theta\left(\tau_{\theta\theta} + \tau_{\phi\phi}\right) \tag{2}$$

$$\frac{\partial(r^2\sin\theta\rho u_\theta)}{\partial t} + \frac{\partial(r^2\sin\theta\rho u_r u_\theta)}{\partial r} + \frac{\partial(r\sin\theta\rho {u_\theta}^2)}{\partial\theta} + r\sin\theta\rho u_r u_\theta = \\ - Sg_\theta + \frac{\partial}{\partial r}\left(r^2\sin\theta\tau_{R\theta}\right) + \frac{\partial}{\partial\theta}\left(r\sin\theta\tau_{\theta\theta}\right) + r\sin\theta\left(\tau_{R\theta} - \cot\theta\tau_{\phi\phi}\right) \tag{3}$$

the viscous stress tensors τ_{RR}, $\tau_{R\theta}$, $\tau_{\theta\theta}$ and $\tau_{\phi\phi}$ are written as:

$$\tau_{RR} = \frac{2}{Re}\frac{\partial u_r}{\partial r}, \quad \tau_{\theta\theta} = \frac{2}{Re}\left[\frac{1}{r}\frac{\partial u_\theta}{\partial\theta} + \frac{u_r}{r}\right], \quad \tau_{\phi\phi} = \frac{2}{Re}\left[\frac{u_r}{r} + \frac{u_\theta\cot\theta}{r}\right], \quad \tau_{R\theta} = \frac{2}{Re}\left[r\frac{\partial}{\partial r}\left(\frac{u_\theta}{r}\right) + \frac{1}{r}\frac{\partial u_r}{\partial\theta}\right]$$

$$\frac{\partial(r^2\sin\theta\rho\Phi)}{\partial t}+\frac{\partial(r^2\sin\theta\rho u_r\Phi)}{\partial r}+\frac{\partial(r\sin\theta\rho u_\theta\Phi)}{\partial\theta}=\frac{\partial}{\partial r}\left(\frac{r^2\sin\theta}{Le_i}T^n\frac{\partial\Phi}{\partial r}\right)+\frac{\partial}{\partial\theta}\left(\frac{\sin\theta}{Le_i}T^n\frac{\partial\Phi}{\partial\theta}\right) \tag{4}$$

The closure for the system above is provided by the dimensionless equation of state of the gas, written as $\rho T=1$. The buoyancy force in Eqs. (2) and (3) is represented through the therms $Sg_r=r^2\sin\theta\cos\theta\left(\rho-\rho_\infty\right)/Fr^2$ and $Sg_\theta=r^2\sin^2\theta\left(\rho-\rho_\infty\right)/Fr^2$ in the radial and polar directions, respectively. The parameters $Fr=u_c^*/\sqrt{g^*\mathrm{a}^*}$, $Re=u_c^*\mathrm{a}^*/\nu^*$ and Le_i are Froude, Reynolds and Lewis of the i specie numbers, respectively, in which $i=F$ for fuel and $i=O$ for oxidant and ν^* is the viscosity. In the present model, is assumed that the combustion process occurs under condition of Damköhler number infinitely large ($Da\gg 1$). In other words, the reaction characteristic time is infinitely smaller than any mechanical characteristic time. Thus, the reactants can not coexist, i.e., the flow field is divided in two domains separated by a reaction sheet. In the fuel domain $y_O=0$ the oxygen concentration is zero. In the oxygen domain, $y_F=0$. Both reactants have zero concentration at the flame, where the chemical reaction takes place. Equation (4), describes the temperature and the oxygen and fuel mass fractions by determining the mixture fraction and the enthalpy excess functions in the fuel region and in the oxygen region (Shvab-Zel'dovich formulation) (Fachini, 1999). Where, $\Phi=Z$ for the mixture fraction defined by

$$Z=Sy_F-y_O+1,\quad S=sLe_O/Le_F, \tag{5}$$

or $\Phi=H$ for the enthalpy excess defined by

$$H=(S+1)\frac{Le_FT}{Q}+y_O+y_F \tag{6}$$

in which $s\equiv\nu/y_{O\infty}$, ν is the mass of oxidant consumed for each unit of mass of fuel in the condition of stoichiometric reaction and $Q\equiv Q^*/c_p^*T_b^*$ is the heat combustion.

The boundary conditions are given as follows:

Droplet surface: $(0\le\theta\le\pi)$ at $r=1$

$$\rho=\rho_s,\quad T=T_b,\quad u_r=1,\quad u_\theta=0,\quad Z=S+1,\quad H=(S+1)\frac{T_b}{Q}+1 \tag{7}$$

in which the subscript "s" stand for condition at the droplet surface.

Downstream: $(0\le\theta\le\pi/2)$ at $r=r_\infty$

$$\rho=\rho_\infty,\quad T=T_\infty,\quad \frac{\partial u_\theta}{\partial r}=0,\quad Z=0,\quad H=(S+1)\frac{T_\infty}{Q}+1 \tag{8}$$

Upstream: $(\pi/2<\theta\le\pi)$ at $r=r_\infty$

$$\frac{\partial T}{\partial r}=\frac{\partial\rho}{\partial r}=\frac{\partial u_\theta}{\partial r}=\frac{\partial Z}{\partial r}=\frac{\partial H}{\partial r}=0 \tag{9}$$

the radial velocity component u_r is estimated by mass conservation, Eq. (1) for $(0<\theta\le\pi)$ at $r=r_\infty$.

Symmetrical axis: $\theta=0$ and π for $0\le r\le r_\infty$

$$\frac{\partial T}{\partial\theta}=\frac{\partial\rho}{\partial\theta}=\frac{\partial u_r}{\partial\theta}=\frac{\partial u_\theta}{\partial\theta}=\frac{\partial Z}{\partial\theta}=\frac{\partial H}{\partial\theta}=0 \tag{10}$$

3. NUMERICAL SOLUTION

The equations are discretized by finite difference method. To obtain steady-state solution, an artificial time-dependent (Euler-Forward) is employed in the Eqs. (1)-(4) The numerical solution follows the sequence: (a) a analytical solution for the spherical flame regime and zero velocity are provided as a initial condition, (b) a first estimative for density ρ_1 is obtained by mass conservation, (c) the velocities components u_r and u_θ are obtained by Eqs. (2) and (3), (d) the mixture fraction Z, Eq. (4), provides the estimative for species y_F, y_O, (e) the temperature T is obtained by excess enthalpy H, Eq. (4), (f) the a new estimative for density ρ_2 is obtained by equation of state, (g) an average between 1 and 2 is obtained $\rho_{new}=0.5(\rho_1+\rho_2)$ finally, this numerical procedure is recursively repeated until the solution reach the steady state by the global convergence criteria as follows: For $\phi_{i,j}\ge\phi^{max}\times10^{-3}$, $\left|(\phi_{i,j}-\phi_{i,j}^{prev})/\phi_{i,j}\right|\le\times10^{-6}$ otherwise, $\left|(\phi_{i,j}-\phi_{i,j}^{prev})/\phi^{max}\times10^{-3}\right|\le\times10^{-6}$; where ϕ is ρ, u_r, u_θ, Z and H; the superscript (prev) indicates the value at the previous iteration; and ϕ^{max} is the maximum variable value in the given phase.

4. RESULTS AND DISCUSSION

The results are presented for a spheric porous droplet at constant radius. The fuel used in the present model is the n-heptane. Fuel vapor is injected in the ambient atmosphere at boiling temperature T_b with constant velocity $U_r = 1$. The droplet is exposed at different ambient temperatures ($T_\infty = 3$ and $T_\infty = 6$), in order to analyze the influence of buoyancy force at normal gravity $g = 9.8\ m/s^2$ condition.

To test mesh independence the simulation was run at different resolutions. Figure 2 shows the results for temperature profile at $\theta = 0, \pi/2$ and π for two meshes with resolution of 60 x 180 and 300 x 320 points. The results indicate that the solution obtained by the present model is not dependent of mesh resolution.

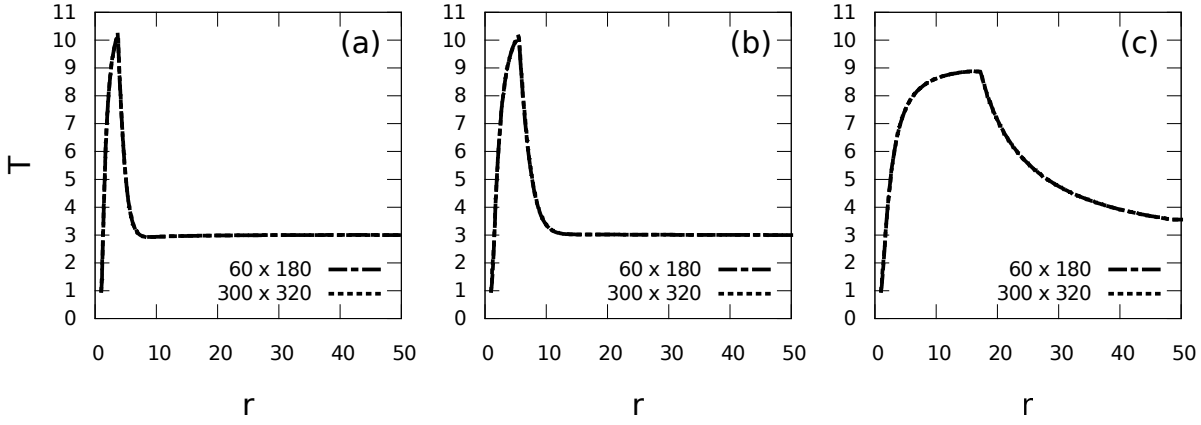

Figure 2: **Temperature profile with $T_\infty = 3$ and $g = 9.8\ m/s^2$: (a) Downstream ($\theta = 0$), (b) Center ($\theta = \pi/2$) and (c) Upstream ($\theta = \pi$).**

Figures 3-a and 3-b show the gas-phase streamlines surrounding the droplet for $g = 9.8\ m/s^2$ and $g = 0\ m/s^2$ case, respectively. For the normal gravity case, flow directions are influenced by natural convection due the presence of the buoyancy term in the conservation equation. In contrast, for the case without gravity the buoyancy term is neglected and there is no natural convection acting in the flow field.

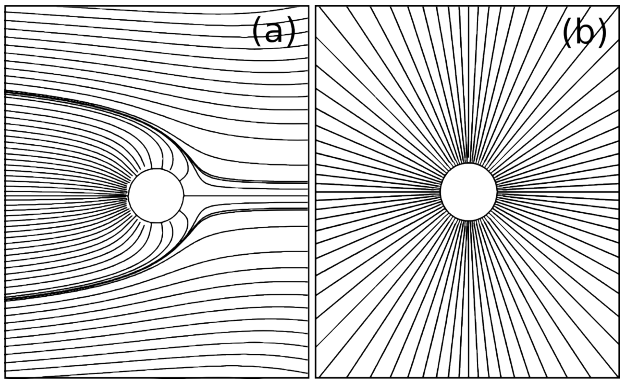

Figure 3: **Streamlines for $T_\infty = 3$: (a) $g = 9.8\ m/s^2$, (b) $g = 0\ m/s^2$.**

Figures 4-a, 4-b and 4-c show the density distribution along the upstream ($\theta = \pi$), center ($\theta = \pi/2$) and downstream ($\theta = 0$) axis. Figure 4-a shows the condition $g = 0$ and temperature $T_\infty = 3$. As expected, the density stays the same in all axes due to the spherical symmetry of the flow. On other hand, in normal gravity cases (Fig. 4-b) at same ambient temperature $T_\infty = 3$, density is lower on upstream axis than the downstream center axis. Figure 4-c shows the case of high temperature. The difference of density between upstream and the two other axes is reduced due the decrease in the gradient of the temperature as a consequence of the reduction of buoyancy force.

Figures 5-a, 5-b and 5-c present the velocity distribution along the upstream ($\theta = \pi$), center ($\theta = \pi/2$) and downstream ($\theta = 0$) axis. In accordance with the density, the flow is accelerated at place of low density. For condition $g = 0$, Fig.5-a, the velocity is null in the region far from the droplet. In the case of $g = 9.8m/s^2$, Figs. 5-b and 5-c, the flow is accelerated in the direction from downstream to upstream according with natural convection. Also, the velocity is null due to the the stagnation point at the downstream in the flux. The stagnation point is due to the injection fuel at the droplet surface in direction opposed to the flow induced by buoyancy force. In addition, the flow velocity decrease with the increase of the ambient temperature. Figure 6 shows the flame position. The flame shape clearly show the influence of ambient temperature. When the ambient temperature increase, the temperature gradient is reduced and the flame tends to become

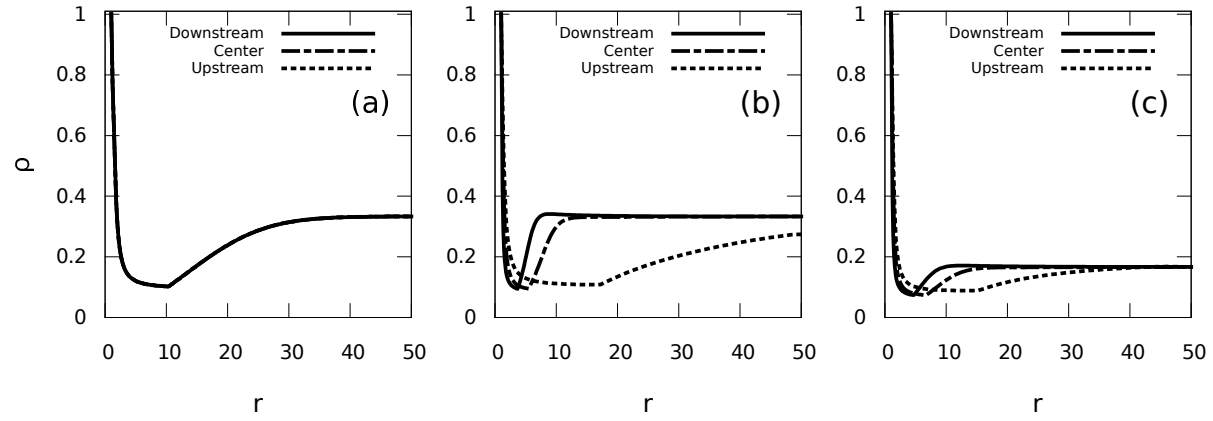

Figure 4: **Distribution of density for (a)** $T_\infty = 3$ **and** $g = 0\ m/s^2$**, (b)** $T_\infty = 3$ **and** $g = 9.8\ m/s^2$**, (c)** $T_\infty = 6$ **and** $g = 9.8\ m/s^2$**.**

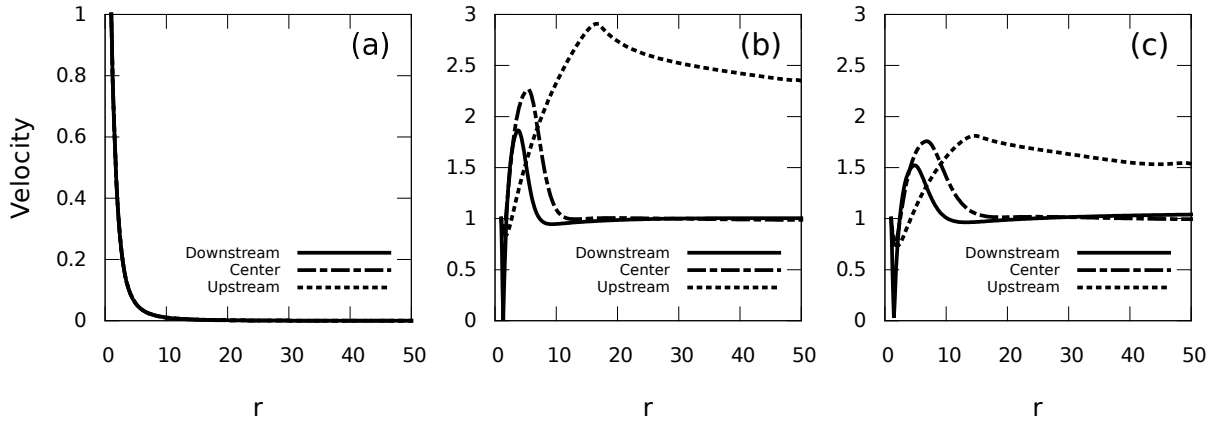

Figure 5: **Distribution of velocity for (a)** $T_\infty = 3$ **and** $g = 0\ m/s^2$**, (b)** $T_\infty = 3$ **and** $g = 9.8\ m/s^2$**, (c)** $T_\infty = 6$ **and** $g = 9.8\ m/s^2$**.**

with spherical symmetry. A hypothetic case with ambient at high temperature $T_\infty = 10$ (10 times the boiling temperature, about $3700\ K$). In this case is possible see that the flame is almost spherical. Figure 7 shows the mass fraction of fuel

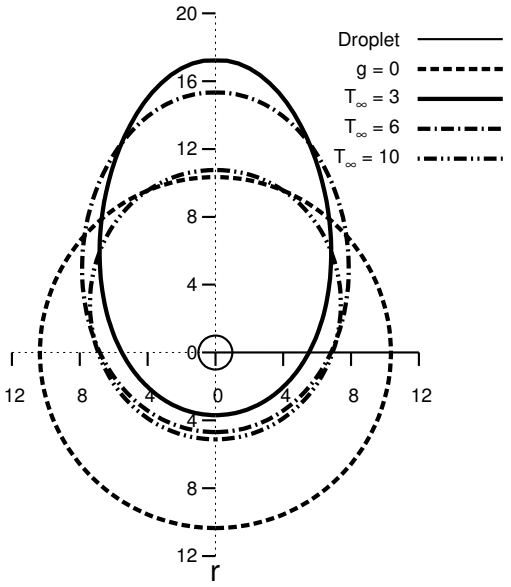

Figure 6: **Flame position at different ambient temperatures.**

and oxidant obtained by the solution of mixture fraction along the upstream ($\theta = \pi$), center ($\theta = \pi/2$) and downstream ($\theta = 0$) axis. As expected the fuel and oxidant are totally consumed at flame position, in the left side is the fuel and right side is the oxidant. In the upstream axis in the normal gravity condition, Figs. 7-b and 7-c, the mass fraction of oxidant is lower than unity (about 0.8). Its can be explained due the flow of the combustion products in the upstream direction.

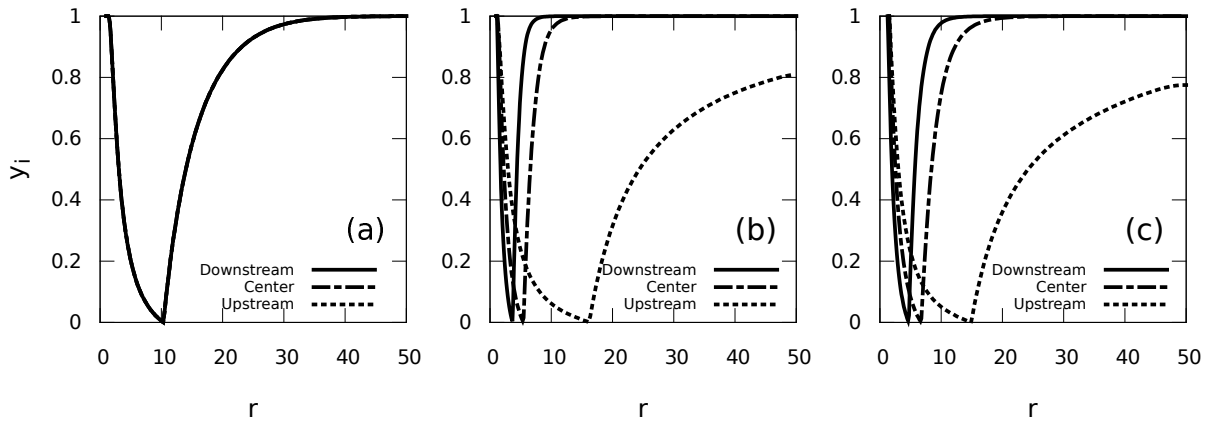

Figure 7: **Distribution of mass fraction for (a)** $T_\infty = 3$ **and** $g = 0\ m/s^2$**, (b)** $T_\infty = 3$ **and** $g = 9.8\ m/s^2$**, (c)** $T_\infty = 6$ **and** $g = 9.8\ m/s^2$**.**

Figure 8-a shows the temperature field for condition of $g = 0$ and $T_\infty = 3$, the spherical symmetry is evidenced. The condition of normal gravity $g = 9.8$ at $T_\infty = 3$, Fig. 8-b, and $T_\infty = 6$, Fig. 8-c, show the influence of the temperature in the buoyancy force. According to previous analysis the flame tends to spherical geometry when the ambient temperature is increased. But the flame shape is not concentric with the droplet as shown in the zero gravity condition Fig. 8-a.

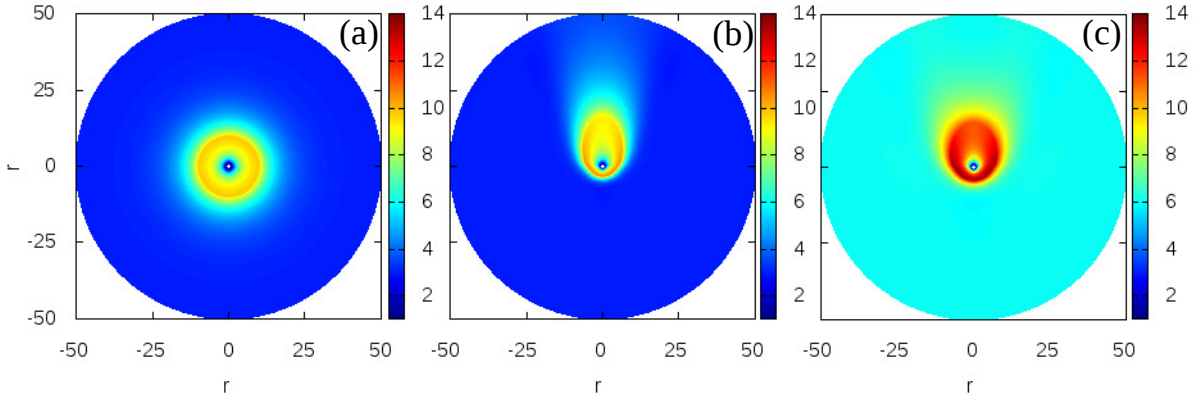

Figure 8: **Temperature field (a)** $g = 0$**, (b)** $g = 9.8$ **and** $T_\infty = 3$**,(c)** $g = 9.8$ **and** $T_\infty = 6$**.**

5. CONCLUSIONS

Combustion of porous sphere droplet with h-heptane was analyzed by numerical solution under normal and zero-gravity conditions with different ambient temperature. The effect of buoyancy was analyzed by the change of the gravity source term on momentum conservation equations. The source depends on the difference between the density in the domain and the density far from the droplet ($\rho - \rho_\infty$). Thus the acceleration of the hot gases is induced by the gradient of the temperature in the ambient. The main objective of the present investigation was analyze the ambient condition that can reproduce spherical flame. The results presented in this work shows that when the ambient temperature increases, the flame radius decrease and became approximately spherical and not elliptical. However, the flame shape is not concentric with the droplet, as observed in microgravity condition $g = 0$.

6. REFERENCES

Chauveau, C., Birouk, M. and Gökalp, I., 2011. "An analysis of the d 2-law departure during droplet evaporation in microgravity". *International Journal of Multiphase Flow*, Vol. 37, No. 3, pp. 252–259.

Choi, M.Y. and Kyeong-Okk, L., 1996. "Investigation of sooting in microgravity droplet combustion". In *Symposium (International) on Combustion*. Elsevier, Vol. 26, pp. 1243–1249.

Dietrich, D.L., Haggard, J., Dryer, F.L., Nayagam, V., Shaw, B.D. and Williams, F.A., 1996. "Droplet combustion experiments in spacelab". In *Symposium (International) on Combustion*. Elsevier, Vol. 26, pp. 1201–1207.

Dietrich, D.L., Nayagam, V., Hicks, M.C., Ferkul, P.V., Dryer, F.L., Farouk, T., Shaw, B.D., Suh, H.K., Choi, M.Y., Liu, Y.C. *et al.*, 2014. "Droplet combustion experiments aboard the international space station". *Microgravity Science and Technology*, Vol. 26, No. 2, pp. 65–76.

Eigenbrod, C., 1999. "European microgravity combustion science, from drop towers to the space station". *Annales Academia Scientiarium et Artium Europea*.

Fachini, F.F., 1999. "An analytical solution for the quasi-steady droplet combustion". *Combustion and flame*, Vol. 116, No. 1, pp. 302–306.

Jiang, T.L., Chen, W.S., Tsai, M.J. and Chiu, H.H., 1995. "A numerical investigation of multiple flame configurations in convective droplet gasification". *Combustion and flame*, Vol. 103, No. 3, pp. 221–238.

King, M.K. and Ross, H.D., 1998. "Overview of the nasa microgravity combustion program". *AIAA journal*, Vol. 36, No. 8, pp. 1337–1345.

Manzello, S.L., Choi, M.Y., Kazakov, A., Dryer, F.L., Dobashi, R. and Hirano, T., 2000. "The burning of large n-heptane droplets in microgravity". *Proceedings of the Combustion Institute*, Vol. 28, No. 1, pp. 1079–1086.

Pope, D.N. and Gogos, G., 2005. "Numerical simulation of fuel droplet extinction due to forced convection". *Combustion and Flame*, Vol. 142, No. 1, pp. 89–106.

Yozgatligil, A., Park, S.H., Choi, M.Y., Kazakov, A. and Dryer, F.L., 2007. "Influence of oxygen concentration on the sooting behavior of ethanol droplet flames in microgravity conditions". *Proceedings of the Combustion Institute*, Vol. 31, No. 2, pp. 2165–2173.

7. RESPONSIBILITY NOTICE

The authors are the only responsible for the printed material included in this paper.